

## **Sea Level Variations along the U.S. Pacific Northwest Coast: Tectonic and Climate Controls**

Author(s): Paul D. Komar, Jonathan C. Allan\*, and Peter Ruggiero

Source: Journal of Coastal Research, 27(5):808-823. 2011.

Published By: Coastal Education and Research Foundation

DOI: <http://dx.doi.org/10.2112/JCOASTRES-D-10-00116.1>

URL: <http://www.bioone.org/doi/full/10.2112/JCOASTRES-D-10-00116.1>

---

BioOne ([www.bioone.org](http://www.bioone.org)) is a nonprofit, online aggregation of core research in the biological, ecological, and environmental sciences. BioOne provides a sustainable online platform for over 170 journals and books published by nonprofit societies, associations, museums, institutions, and presses.

Your use of this PDF, the BioOne Web site, and all posted and associated content indicates your acceptance of BioOne's Terms of Use, available at [www.bioone.org/page/terms\\_of\\_use](http://www.bioone.org/page/terms_of_use).

Usage of BioOne content is strictly limited to personal, educational, and non-commercial use. Commercial inquiries or rights and permissions requests should be directed to the individual publisher as copyright holder.



www.cerf-jcr.org

# Sea Level Variations along the U.S. Pacific Northwest Coast: Tectonic and Climate Controls

Paul D. Komar<sup>†</sup>, Jonathan C. Allan<sup>\*‡</sup>, and Peter Ruggiero<sup>§</sup>

<sup>†</sup>College of Oceanic & Atmospheric Sciences  
Oregon State University  
Corvallis, OR 97331

<sup>‡</sup>Coastal Field Office  
Oregon Department of Geology and Mineral  
Industries  
P.O. Box 1033, Newport, OR 97365  
jonathan.allan@dogami.state.or.us

<sup>§</sup>Department of Geosciences  
Oregon State University  
Corvallis, OR 97331

## ABSTRACT

Komar, P.D.; Allan, J.C., and Ruggiero, P., 2011. Sea level variations along the U.S. Pacific Northwest coast: tectonic and climate controls. *Journal of Coastal Research*, 27(5), 808–823. West Palm Beach (Florida), ISSN 0749-0208.

Analyses of the progressive multidecadal trends and climate-controlled annual variations in mean sea levels are presented for nine tide-gauge stations along the coast of the U.S. Pacific Northwest: Washington, Oregon, and Northern California. The trends in relative sea levels are strongly affected by the tectonics of this region, characterized by significant alongcoast variations in changing land elevations measured by benchmarks and global positioning system data. These combined data sets document the existence of both submergent and emergent stretches of shore. The Pacific Northwest sea levels are also affected by variations in the monthly mean seasonal cycles, with its extreme water levels occurring in the winter during strong El Niños. To quantify this climate control and to derive improved multidecadal sea-level trends, separate evaluations of the winter and summer-averaged measured water levels have been undertaken. The resulting pair of linear regressions for each tide gauge shows a consistent difference in the mean water levels over the years, at their highest during the winters, reflecting the total magnitude in the seasonal cycle of water levels. Of importance, the degree of scatter in the summer averages is reduced compared with the annual averages, yielding sea-level trends that generally have the highest statistical significance. In contrast, the winter records emphasize the extreme water levels associated with strong El Niños, yielding a predictive correlation with the Multivariate El Niño/Southern Oscillation Index. Both trends in relative sea levels and extremes in the winter monthly elevations produced by El Niños are important to the Pacific Northwest coastal hazard assessments, combining with the multidecade increase in wave heights measured by buoys. With these multiple processes and their climate controls, the erosion hazards are projected to significantly increase in future decades.

**ADDITIONAL INDEX WORDS:** *El Niño, Oregon, Washington, California, relative sea level, coastal land elevation, global positioning system (GPS), coastal hazards, coastal erosion.*



www.JCRonline.org

## INTRODUCTION

A documentation of the progressive trends and annual variations in mean sea levels is basic to understanding the erosion and flooding hazards along coastal margins and to projecting the enhanced impacts expected during the 21st century due to Earth's changing climate. The rise in the global mean sea level was clearly important to the 20th century coastal impacts, with that increase evaluated to have averaged approximately 1.7 mm/y (Church and White, 2006; Holgate, 2007; Miller and Douglas, 2004). The reports by the Intergovernmental Panel on Climate Change (IPCC) projected that the rates of rising sea levels will likely accelerate during this century in response to global warming (Bindoff *et al.*, 2007). However, even the more extreme IPCC projections are already considered by some researchers to be on the low side, based on recent analyses of the patterns, rates, and processes driving glacial melting (Hansen, 2007; Pfeffer, Harper, and Neel, 2008). Along coastal margins, the combination of the global rise

in sea level (its local eustatic rate) and local changes in land elevations is significant to the resulting erosion and flooding, the relative sea level (RSL) that is directly measured by tide gauges.

Assessments of the trends and variations in sea levels are important to our ongoing investigations of erosion and flooding hazards along the coast of the U.S. Pacific Northwest (PNW), the ocean shores of Washington, Oregon, and the northernmost portion of California (south to Cape Mendocino). The tide-gauge records of this region are strongly affected by its tectonics, this being a zone of collision between Earth's tectonic plates and producing significant alongcoast variations in land-elevation changes. While some stretches of the coast are being submerged by the net rise in RSL, other areas are presently experiencing uplift at faster rates than the increase in sea level, resulting in an emergent coast. However, if the projections of accelerated rates of sea-level rise are reasonably accurate, later in this century the eustatic rise can be expected to exceed the tectonic uplift, inducing property erosion in areas where it is now minor to nonexistent (Ruggiero, 2008).

Another challenge in analyzing the PNW sea-level records is its variable climate, the most important aspect of which is

DOI: 10.2112/JCOASTRES-D-10-00116.1 received 5 August 2010; accepted in revision 9 December 2010.

© Coastal Education & Research Foundation 2011

occurrences of major El Niños that elevate mean sea levels by tens of centimeters throughout the winter and have largely been responsible in recent decades for episodes of beach and property erosion (Allan and Komar, 2006; Komar, 1997). This climate cycle also produces significant scatter in the annual mean sea levels derived from tide-gauge records, reducing the statistical significance of the linear regressions undertaken to determine the trends of change in RSLs, particularly since the majority of those records are approximately 40 years or shorter.

Here we report on analyses undertaken to reduce this scatter in the sea-level trends by applying revised analysis procedures and by investigating the El Niño–La Niña climate controls on the tide-gauge records, which largely accounts for that scatter. The results are both improved assessments of the rates of changing sea levels along the coast of the PNW and improved understanding of the magnitudes of increased water levels that occur during strong El Niños. The substantial range in trends and variations in sea levels along this coast is a primary factor in the degrees of its erosion impacts, as are the climate controls on the increasing storm intensities and wave heights measured by buoys since the 1970s (Allan and Komar, 2000, 2006; Ruggiero, Komar, and Allan, 2010). The products of this study are important to the management of the PNW coast, directed toward a reduction of the erosion and flooding impacts anticipated in the future due to Earth's changing climate.

### TECTONICS AND CLIMATE OF THE PACIFIC NORTHWEST

The coast of the PNW is tectonically active, being a collision coast in the classification by Inman and Nordstrom (1971), referred to as the Cascadia Subduction Zone. As shown in Figure 1, the PNW is the region where the oceanic Juan de Fuca and Gorda plates are moving northeasterly at a relative rate of about 4 cm/y, colliding with and being subducted beneath the continental North American plate. The most recent subduction earthquake occurred on 26 January 1700, when an estimated magnitude 9 earthquake generated a catastrophic tsunami that swept across this coast (Atwater, 1987; Atwater and Hemphill-Haley, 1997; Kelsey *et al.*, 2005; Nelson, Kelsey, and Witter, 2006; Satake *et al.*, 1996; Witter, Kelsey, and Hemphill-Haley, 2003). Geologic investigations of sequences of buried marshes and tsunami sands documented the occurrences of multiple earthquakes spanning thousands of years, with an average recurrence interval of 300 to 500 years. However, recent studies indicate that subduction earthquakes have been more frequent at the lower latitudes of southern Oregon and northern California, with longer periods between events at the higher latitudes of northern Oregon and Washington, caused by the partial ruptures of the subduction zone (Goldfinger *et al.*, in press).

Of relevance to this study of sea levels and chronic coastal hazards are the changes in land elevations along this coast that result from its tectonic setting. At the time of the 1700 earthquake, nearly the entire coast abruptly subsided, in some areas by up to 2 m (Leonard *et al.*, 2010; Witter, Kelsey, and Hemphill-Haley, 2003), as a result of the release of the tension within the crust that had been stored while the plates were locked together since the previous subduction earthquake. Of

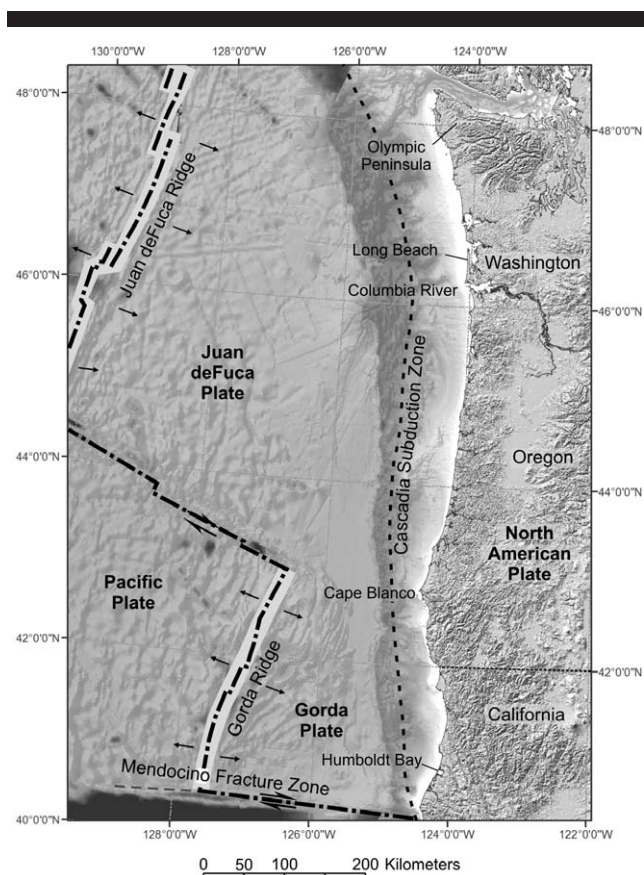


Figure 1. The tectonic setting of the PNW, with the collision and subduction of the ocean plates beneath the continental North American plate.

significance to coastal change, with the plates again being locked and with strain accumulating, the coast is tectonically rising but at varying rates along its length of shore. The resulting land-elevation changes have been documented through analyses of decadal surveys of benchmarks used by surveyors (Burgette, Weldon, and Schmidt, 2009; Mitchell *et al.*, 1994), and with data derived from global positioning system (GPS) stations. In brief, the southern one-third of the Oregon coast is tectonically rising faster than the regional rise in sea level (the eustatic rise in the NE Pacific), so its shores are emergent, whereas along most of the northern half of the Oregon coast the rate of rise in the land elevations has been less, so the measured rates of sea-level rise are close to the eustatic value. As a result, this stretch of shore is slowly submergent, being transgressed by the ocean. At the mouth of the Columbia River, the border between Oregon and Washington, the land is rising at approximately the same rate as the eustatic rise, with the relative change close to zero. Just to the north, along the Long Beach Peninsula of Washington, there appears to again be a net rise in the RSL. Still farther north, along the ocean shore of the Olympic Peninsula of Washington, high rates of uplift have been occurring, with this northernmost portion of the PNW coast also emergent. The resulting regional differences in directions and rates of changing RSLs,



Figure 2. The NOAA tide gauges analyzed in this study.

with stretches of both submergent and emergent shores, are directly reflected in their contrasting impacts from erosion (Komar and Shih, 1993).

Also affecting the mean water levels along the PNW coast are various atmospheric and ocean processes, each of which to varying degrees has its climate controls (Huyer, 1977; Huyer and Smith, 1985; Smith, Huyer, and Fleischbein, 2001). Particularly important are the seasonal variations in the directions and speeds of the shelf currents and the associated occurrences of upwelling during the summer, governed by the changing directions of the coastal winds. Those processes in

turn produce seasonal variations in water temperatures, which are coldest and most dense during the summer, warm and less dense in the winter. This seasonal change in water temperatures results in a parallel cycle of the monthly mean water levels measured by the tide gauges, which is highest during the winter due to the thermal expansion of the warmer water during that season. The occurrence of a major El Niño has a significant effect on the ocean currents, resulting in a reduction in the upwelling so that the water temperatures are warmer than normal during that climate event, temporarily raising sea levels along the PNW coast by tens of centimeters compared with non-El Niño years. Most significant in recent decades in terms of the magnitudes of these processes and in the resulting erosion impacts were the strongest El Niños of 1982–83 and 1997–98.

### TIDE-GAUGE DATA

The data analyzed in this study were derived from nine PNW tide gauges operated by the National Oceanic and Atmospheric Administration (NOAA). The locations of the gauges are identified in Figure 2, and a comparison with the tectonics in Figure 1 demonstrates that the eight coastal sites span the length of shore affected by the subduction of the oceanic plates beneath the continent. The ninth gauge is located within Puget Sound (Seattle), providing an exceptionally long record from a relatively stable site, and was included in this study to develop our analysis methodologies and to provide a comparison with the results from the coastal gauges.

Specifics concerning the tide gauges analyzed in this study are given in Table 1, including their N–S latitudes, environmental locations (*e.g.*, within bays *vs.* along open coast), and the record dates and lengths in years that have been analyzed. Along the coast three of the eight gauges are in open-ocean harbors protected by breakwaters, while the Willapa Bay and Coos Bay tide gauges are within bays but close to the inlets (at Toke Point in Willapa Bay and at Charleston in Coos Bay). The Yaquina Bay gauge is midway along the length of that estuary, 3.8 km from its mouth, while the Astoria gauge on the Columbia River has the most distant inland position of these coastal sites, as it is 23.5 km from the river's mouth.

Table 1 shows that the longest records are available from Seattle (110 years), Neah Bay (75 years), Astoria (85 years),

Table 1. Pacific Northwest NOAA tide gauges.

Gauge Site	Latitude	Gauge Location	Record Interval	Years
Washington				
Seattle	47.60	Puget Sound	Jan. 1899–Dec. 2009	110
Neah Bay	48.37	Open coast harbor	Aug. 1934–Dec. 2009	75.4
Willapa Bay	46.71	Toke Point near inlet	Oct. 1968–Dec. 2009	41.3
Oregon				
Astoria	46.22	Columbia River	Feb. 1925–Dec. 2009	84.9
Yaquina Bay	44.63	South Beach	Feb. 1967–Dec. 2009	41.9
Coos Bay	43.35	Charleston harbor	April 1970–Dec. 2009	38.7
Port Orford	42.74	Open coast harbor	Oct. 1977–Dec. 2009	32.3
California				
Crescent City	41.75	Open coast harbor	Jan. 1933–Dec. 2009	77.0
Humboldt Bay	40.77	North spit	Sep. 1977–Dec. 2009	31.3

and Crescent City (77 years), time spans that are sufficient to yield assessments of their trends of changing RSLs despite the scatter of the data produced by El Niños. In contrast, the records from the other gauges are on the order of only 30 to 40 years, generally considered to be too short for assessments of trends in attempts to derive a value for the 20th-century global rise in sea level (Douglas, 2001; Pugh, 2004). Furthermore, these 30- to 40-year records also correspond primarily to the warm phase of the Pacific Decadal Oscillation (PDO) when major El Niños were prominent, and this has resulted in an enhanced degree of data scatter, making it difficult to derive statistically meaningful values for the rates of sea-level change. However, these short tide-gauge records are important in our applications to derive hazard-zone assessments along this coast. As a result, our analysis methodologies described in the following section are directed toward smoothing the data to obtain statistically improved multidecadal trends, and a separate methodology is developed to account for the winter extremes caused by the range of El Niño–La Niña climate events.

The water-level data were obtained from the National Ocean Service (2009), consisting of both the hourly and the monthly mean water levels for each year of record. A criterion was adopted that if a single month of data was missing, that year would be excluded in analyses of the trends of annual averages and would not be included in analyses of the seasonal trends and variations (winter *vs.* summer), the methodology discussed in the following section.

Special issues relate to the analyses of the Yaquina Bay and Astoria tide gauges. In their investigation of the PNW tectonics and land-elevation changes based on benchmark data, Burgette, Weldon, and Schmidt (2009) used the tide-gauge records and in doing so investigated the stabilities of the primary benchmarks to which the gauge records are related. They found that one of the primary benchmarks for the Yaquina Bay gauge is positioned on unstable ground. Between 1967 when the gauge was installed and 1972, the benchmark subsided at a rate of 4.99 mm/y, decreasing to 1.59 mm/y between 1972 and 1996; since 1996, no evidence was found for the occurrence of additional subsidence. The subsidence of that benchmark is also indicated by our analyses of the relative sea-level trends for the Yaquina Bay gauge, supporting their conclusion that any assessment of the rate of change needs to be corrected. To that end, we adjusted the analyses of the Yaquina Bay tide-gauge record using the variable slope adjustment factors identified by Burgette, Weldon, and Schmidt (2009). There are also issues with the Astoria gauge located in the Columbia River, which has been similarly unstable, but in particular there are problems with the data due to the effects of the dams on that river. The operation of those dams has strongly influenced the river discharges, affecting the monthly mean sea levels recorded by the gauge during the months of May through July. Accordingly, the analyses we undertook omitted the data for those months.

## ANALYSIS METHODOLOGIES

The objective of our analyses of the PNW tide-gauge records is first to derive the best possible assessments of the

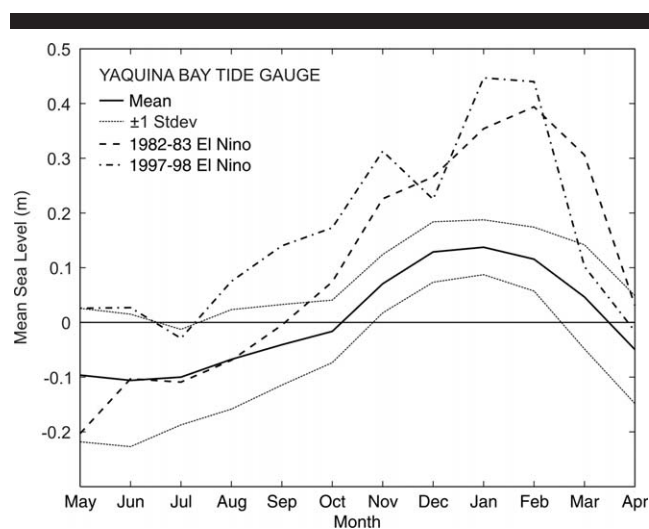


Figure 3. Seasonal cycles of the monthly mean water levels based on data from the Yaquina Bay tide gauge, its long-term average cycle, and extremes during major El Niños.

progressive multidecadal trends in RSLs from the coastal gauges and second to develop an analysis procedure that will document the extremes in the winter monthly mean sea levels caused by El Niños, extremes that are important in causing episodes of erosion and flooding. A determination of the long-term trend with the greatest statistical significance requires a methodology that reduces the scatter of the water-level variations within the time series, whereas the approach taken in this study to document the El Niño extremes focuses on the highest monthly winter water elevations, which can serve as the basis for correlations with the magnitudes within the El Niño–La Niña range of climate events.

Our analyses of the PNW tide-gauge records begin with a determination of the long-term average seasonal cycle of monthly mean water elevations measured over the decades. This average variation is important in comparisons with the elevated water levels during strong El Niños. The example in Figure 3 is based on the record from Yaquina Bay, central to the study area. The records from the other gauges are closely similar in the magnitudes and timing of the seasonal variations. As discussed earlier, the highest monthly mean water levels are seen in Figure 3 to occur during the winter months of December through February and the lowest are in the summer, with a total difference in seasonal water levels on average of about 0.2 m. Also included in Figure 3 are the more extreme seasonal cycles that occurred during the strongest El Niños of 1982–83 and 1997–98, when the monthly mean water levels were approximately 0.5 m higher during the winter than in the previous summer, more than double the normal cycle. These extreme winter water levels during major El Niños are important to erosion and flooding along the PNW coast and are the focus of our analyses in this paper.

On most other coasts (*e.g.*, southern California), the seasonal cycles of monthly mean water levels are essentially the inverse of those found in the PNW, the water levels on those coasts tending to be dominated by solar heating so that the water

temperatures are warmest during the summer to early fall, producing the highest water levels due to its thermal expansion. The reversed seasonal dependence seen in Figure 3 for the PNW is due largely to the occurrence of upwelling during the summer that brings deep cold water to the surface, whereas the water during the winter is warmer and less dense. In addition, during the winter the prevailing winds produce a northward-flowing current, with the Coriolis force tending to turn that current to the right toward the coast, so the geostrophic cross-current balance also contributes to the rise in sea levels along the shore during the winter. Both factors become significantly stronger during El Niños, hence the extreme elevated winter water levels during that climate event (Figure 3).

With exceptionally high mean sea levels occurring along the PNW coast during El Niños, but with the cold water of La Niñas depressing the water levels, the variations from year to year in this range of climate events is the primary factor in producing the data scatter that reduces the statistical significance of trends for the multidecadal change in RSLs, derived from the tide-gauge records (Allan and Komar, 2006). Therefore, it has been necessary to smooth the data to reduce those year-to-year variations that are significantly greater in the PNW tide-gauge records than generally found for other coasts. However, while smoothing the data, it is important that the integrity of the measured tides and their averages be retained in terms of the magnitudes of the water elevations for them to be applicable in our hazard assessments. Accordingly, we chose not to smooth the data by “correcting” it for variations in atmospheric pressures or by using advanced statistical methods such as empirical orthogonal function analyses employed by some investigators.

The traditional methodology to determine the decadal trends simply involved calculating the annual averages of the hourly measured tides. This degree of averaging yields one value for the mean sea level each year, which eliminates the seasonal cycle but allows the extremes due to El Niños to still be represented by peaks in annual mean water levels experienced along the coast, evident in our earlier analyses of the PNW records based on annual averages (Allan and Komar, 2006). However, a methodology now commonly employed to determine decadal trends is to base the analysis on all monthly mean values, but with the long-term average seasonal cycles having been removed (*e.g.*, Zervas, 2009). While the regressions are thereby based on far more data points, 12 *per* year rather than 1 annual average, it is not immediately obvious whether that approach results in a greater degree of smoothing and improved regression statistics.

To resolve this uncertainty as to which methodology to employ in analyzing the PNW tide-gauge data, we undertook comparisons based on the century-long Seattle data, with the results graphed in Figure 4. The topmost panel plots the raw monthly mean values obtained from the NOAA website, while the second panel follows the procedure of removing the long-term average seasonal cycle for the Seattle gauge, which is similar to that illustrated in Figure 3 for Yaquina Bay except that the amplitude of change between summer and winter is smaller (0.15 m). The third panel in Figure 4 graphs the annual mean sea levels. The relative degrees of smoothing in the

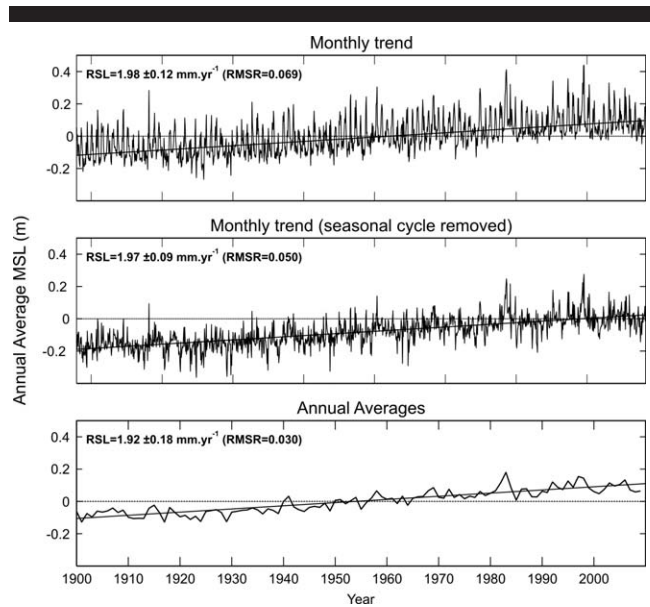


Figure 4. Trends in relative mean sea levels for the Seattle tide gauge, comparing different analysis methodologies based on monthly versus annual averages.

successive graphs are visually apparent. The procedure of subtracting the long-term seasonal cycle reduced the scatter compared with analyzing the raw monthly mean values, but the greatest degree of smoothing is achieved in the graph of the annual averages. The statistics for this series of regressions are compared later in this section, confirming the visual assessments.

While the goal of the analyses in Figure 4 was to reduce the year-to-year variations that are mostly due to the El Niño–La Niña range of climate events, the objective being to derive improved assessments of the long-term trends in RSLs, a different analysis methodology is needed to emphasize the range of water level variations to evaluate their extremes during El Niños. The approach we developed is based on separate evaluations of the mean water levels during winter and summer as illustrated in Figure 5, again with data from the Seattle gauge. Here, “winter” is defined as the combined average tide level measured over a 3-month period around the peak of the seasonal maximum in winter water levels, typically the months of December through February, as seen in Figure 3 for the Yaquina Bay seasonal cycle. Similarly, “summer” water levels reflect the combined average tide level measured over a 3-month period centered on the seasonal minimum, typically May through August, when water levels also tend to be less variable.

Figure 5 shows for the Seattle record that the elevations for the winter are systematically displaced 0.15 m above those for the summer according to their respective regression lines, reflecting the seasonal change in water levels from summer to winter in Puget Sound. By focusing on the highest water levels reached during the winter, the graph for that season emphasizes the extremes during major El Niños. The peaks for the 1982 and 1997 major events are most prominent in the

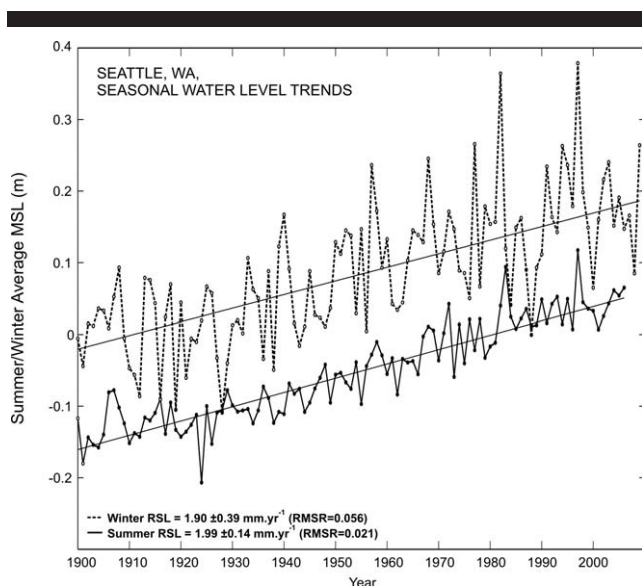


Figure 5. The trends of winter and summer monthly mean sea levels measured by the Seattle tide gauge.

diagram. Furthermore, Figure 5 documents how those levels systematically achieved higher elevations over the decades, with the actual magnitudes of the water levels in 1983 and 1997 having resulted from the combined effects of the enhanced levels attributable to the El Niño processes and the global rise in sea level.

In the seasonal analysis of Figure 5, the data scatter for the summer has been reduced compared with the annual averages by eliminating the winter measurements and their high degrees of variation caused by El Niños; of note is the absence of pronounced water-level peaks in the summer plot associated with the major 1982–83 and 1997–98 El Niños, in contrast with the graph for the winter. In addition, some of the smoothing in the summer graph can be attributed to the absence of storms and their elevated water levels due to the storm surge. This is particularly important in analyses of the coastal tide gauges. Visually, the analysis in Figure 5 of the summer monthly mean water levels for the Seattle record appears to have yielded a greater degree of smoothing than that achieved by the methodologies tested in Figure 4, including that based on the annual averages where the winter measurements are included.

The visual assessments of the degrees of scatter seen in Figures 4 and 5 for the different methodologies are supported by statistical analyses, with the results summarized in Table 2. The most direct assessment of the data scatter above and below

the regression lines, free from any potential serial interdependence of the values within the data set, is provided by the calculated root-mean-square residual (RMSR), with the term “residual” referring to the detrended value of the mean water elevation. The range of RMSR values listed in Table 2 for the series of methodologies corresponds closely to their degrees of visible scatter seen in Figure 4, and for the summer record in Figure 5. The largest value of 0.069 m is obtained for the raw monthly means, reflecting its considerable degree of scatter. It is reduced somewhat to 0.050 m by subtracting the average seasonal cycle and reduced by essentially half to 0.030 m in the analysis based on the annual averages. Additional smoothing is obtained in the analysis in which the annual average is based only on the summer tide-gauge data, with an RMSR of 0.021 m for the Seattle record.

Also included in our statistical analyses listed in Table 2 are estimates of the uncertainties of the trends at the 95% confidence level. Although the least squares linear regression analysis yields an accurate measure of the RSL trend determined by the slope of the line, the analysis can substantially underestimate the uncertainty of that trend because the annual or monthly averages can be serially correlated with one another (Holgate, 2007; Zervas, 2001, 2009). The residual mean sea level for each year (or month) should be independent of the residual values estimated for any previous year (month) or any following year (month). According to Zervas (2001), this condition is often untrue for sea-level time series because the predominant residual signal is characterized by an interannual variability (on the order of several years) that is forced by climate phenomena such as the El Niño/Southern Oscillation (ENSO). As a result, there are fewer independent points in the sea-level time series, contributing to the standard error of a linear regression.

To more accurately resolve the degree of uncertainty in our analyses of the PNW tide-gauge records, the time series were analyzed using a lag-1 autocorrelation function (Maul and Martin, 1993; Zervas, 2001). Listed in Table 2 are the results from our calculations of the confidence intervals (CIs) of the trend estimates, based on the assumption that each value of the mean water level (monthly or annual) is independent, followed by the results that account for the serial correlation of the data within each time series. The latter analysis is accommodated by reducing the number of degrees of freedom using the lag-1 autocorrelation of the time series. The serial correlation coefficient ( $r_1$ ) is first determined. When  $r_1 > 0$ , the effective sample size  $\hat{n}$  is less than the original data  $N$  (World Meteorological Organization, 1966) and can be determined from

$$\hat{n} = N[1 - r_1] / [1 + r_1]$$

Table 2. Statistical analyses of the decadal trends in RSLs for the Seattle tide gauge, evaluated from the raw monthly mean values, monthly values with the seasonal cycle removed, annual average, and summer average RSLs.

Analysis Method	Rate of Sea Level Change (mm/y)	$R^2$	RMSR (m)	$N$	CI ( $\pm$ mm/y)	$\hat{n}$	CI ( $\pm$ mm/y)
Raw monthly	1.98	0.45	0.069	1235	0.12	401	0.22
Monthly (seasonal cycle removed)	1.97	0.60	0.050	1224	0.09	656	0.12
Annual	1.92	0.81	0.030	107	0.18	64	0.24
Summer	1.99	0.89	0.021	101	0.14	94	0.15

which accordingly reduces the degrees of freedom in the statistical tests.

As seen in Table 2, the effective sample size  $n$  resulting from the serial correlation of the values within the time series is reduced from the total size  $N$  of the original time series. As expected, the reduction is greatest in the statistical analysis of the raw monthly values, reduced from the original 1235 values for the Seattle record to an effective  $n$  of only 401. By subtracting the average annual seasonal cycle, the  $n$  retained is increased to 656 but is still only about half the original  $N$  data set. In the analysis of the annual averages, the bottom graph in Figure 4, the original 107 value for  $N$  is reduced to  $n$  of 64, so a higher proportion of the time series is retained. Continuing this progression, the analysis limited to the summer months shows by far the highest data retention: the original value of  $N$  is 101, and the reduced  $n$  is 94. These different statistical results that depend on the analysis methodology are understandable in terms of the PNW ocean processes and their expected effects on the serial correlations between the monthly or annual mean water levels. In particular, by limiting the analysis to the summer months, the effects of the El Niño–La Niña range of climate events are nearly eliminated, whereas they have been retained to varying degrees in the other methodologies.

The calculation of the CI depends strongly on the number of data values  $N$  in the original time series. Therefore, in the initial assessments assuming that the values are independent, the calculated CI for the regressions based on the monthly averages are substantially narrower than those for the annual averages since there are 12 times as many months than years in the time series; this despite the greater scatter when having used the monthly averages. However, evident in Table 2 is that with the reduction in  $n$  due to serial correlations, there is an increase in the values of the CI for each of the analysis methodologies, but this reduction in  $n$  is much greater for the analyses based on the monthly mean water levels than the annual averages. In the case of the analysis in which the average seasonal cycle has been subtracted from the monthly averages, the CI values are  $\pm 0.09$  and  $\pm 0.12$  mm/y, respectively for the independent and serially correlated assumptions, the increase for the latter reflecting the significant reduction in the value for  $n$  inherent in that methodology. The analysis of the summer annual averages yields CI values of  $\pm 0.14$  and  $\pm 0.15$  mm/y, there having been little change due to the minimal degree of interdependence within the summer measurements. Its values are now essentially the same as the effective  $\pm 0.12$  mm/y CI value for the analysis based on the monthly averages. Therefore, the gain from basing the analysis on 12 times as much data in the methodology using the monthly averages has been offset by the significantly greater degrees of serial correlation of that data, as well as by its greater scatter, compared with analyses based on annual measures of the mean water levels. In terms of the statistical analyses summarized in Table 2, the regressions based on the annual averages have the greatest levels of significance when we consider both the RMSR and the CI values, with the regressions for the summer monthly averages providing a further improvement over the annual averages.

The regression slopes representing the rate of change of the RSLs in this series of analysis methodologies applied to the

Seattle tide-gauge record range from 1.92 to 1.99 mm/y (Table 2). Considering the varying degrees of data scatter and effective CI uncertainties, this small range of rates essentially represents a nearly identical assessment. This close correspondence can be attributed to the 110-year length of the Seattle tide-gauge record and the reduced variations within Puget Sound caused by El Niños, compared with those on the ocean shore. In the following sections of this paper, we show that the differences are significantly greater in analyses of the short tide-gauge records from the PNW coast, but the results based on the summer averages again provide the greatest degrees of data smoothing and statistical significance.

In summary, the methodology we developed to analyze the trends and variations in monthly mean and annual sea levels for the PNW tide-gauge records is the combination of Figures 4 and 5. All graphs in this analysis of the Seattle time series, whether based on monthly or annual averages, are informative because they documented the variations and extremes in the mean water levels along the PNW coast. Each of the three panels in Figure 4 displays various aspects of the multidecadal variations, in some cases showing the PDO cycles, with the warm phase dominated by major El Niños. In this example for Seattle, the graphs also suggest a tendency for nonlinearity in the trend that departs from the linear regressions. As intended, the methodology in Figure 5 for the winter season provides a documentation of the elevated water levels during that season when the hazards from erosion and flooding are greatest, the most significant of which are the extremes during strong El Niños. Later in this paper, analyses are presented as correlations between the detrended magnitudes of the El Niño water levels and the Multivariate ENSO Index (MEI), yielding a predictive analysis that is important in our management applications. Furthermore, the analyses of the summer monthly mean water levels (Figure 5) in essentially all cases provide a greater degree of smoothing than do the graphs for the annual averages, yielding the statistically best assessments of the progressive trends in RSLs along the PNW coast.

## MULTIDECADAL TRENDS IN ANNUAL AVERAGE SEA LEVELS

Analyses have been completed for the eight coastal tide gauges to determine their multidecadal trends in the RSLs based on the annual averages and for the summer versus winter seasons, applying the methodologies illustrated previously for the Seattle gauge. The results are summarized in Table 3 for the trends derived from the least squares linear regressions, together with the statistical parameters that represent the degrees of data scatter and their CIs, the latter accounting for serial correlations. In this section, the results based on the annual averages are discussed, documenting the tectonic controls on the progressive trends in RSLs affected by the alongcoast variations in land-elevation changes.

The series of graphs in Figure 6 shows the trends of annual averages for the Neah Bay, Yaquina Bay, and Crescent City records, representing the length of coast included in our study. Both Neah Bay and Crescent City are emergent coasts with downward trends of lowered RSLs. Their respective rates according to the regressions are  $-1.85$  and  $-0.78$  mm/y. In

Table 3. Statistical analyses of the decadal trends in RSLs for the PNW tide gauges, evaluated from the annual-average RSLs as illustrated in Figure 4 and for the summer and winter seasonal averages illustrated in Figure 5.

Analysis Method	Rate of Sea Level Change		
	Change (mm/y)	RMSR (m)	CI ( $\pm$ mm/y)
<b>Seattle</b>			
Annual averages	1.92	0.030	0.24
Summer	1.99	0.021	0.15
Winter	1.90	0.056	0.39
<b>Neah Bay</b>			
Annual averages	-1.85	0.032	0.42
Summer	-1.89	0.030	0.35
Winter	-1.97	0.064	0.79
<b>Willapa Bay</b>			
Annual averages**	0.94	0.038	2.14
Summer	1.48	0.027	1.05
Winter**	1.19	0.074	2.59
<b>Astoria</b>			
Annual averages	-0.49	0.039	0.51
Summer	-0.62	0.034	0.35
Winter**	0.11	0.081	0.82
<b>Yaquina Bay<sup>1</sup></b>			
Annual averages**	0.94	0.033	1.44
Summer	1.33	0.030	0.79
Winter**	0.64	0.070	2.06
<b>Coos Bay</b>			
Annual averages**	1.05	0.036	1.59
Summer	1.62	0.032	1.02
Winter**	1.65	0.076	2.62
<b>Port Orford</b>			
Annual averages**	0.63	0.041	3.31
Summer**	1.47	0.041	1.95
Winter**	2.18	0.071	4.52
<b>Crescent City</b>			
Annual averages	-0.78	0.029	0.36
Summer	-1.10	0.039	0.50
Winter	-0.79	0.068	0.77
<b>Humboldt Bay</b>			
Annual averages	4.26	0.036	2.10
Summer	5.30	0.034	1.62
Winter	4.46	0.060	3.62

<sup>1</sup>The rates for Yaquina Bay have been corrected for subsidence of its primary benchmark.

\*\* denotes slope not significantly different from zero, RMSr = root-mean-square residual.

contrast, there is a positive trend of increasing RSLs recorded by the Yaquina Bay gauge on the mid-Oregon coast, with its regression rate being 0.94 mm/y. Although this area is therefore submergent, it must also be experiencing tectonic uplift, but its rate of increasing land elevations is less than at Neah Bay and Crescent City. As discussed later, these trends in RSLs for the longest tide-gauge records are in reasonable agreement with the results from analyses of land-elevation changes based on resurveys of benchmarks and from GPS records along the coast.

The shorter tide-gauge records from Willapa Bay and Coos Bay are graphed in Figure 7. Both are on the order of 40 years in length and show trends of increasing RSLs, the rates of

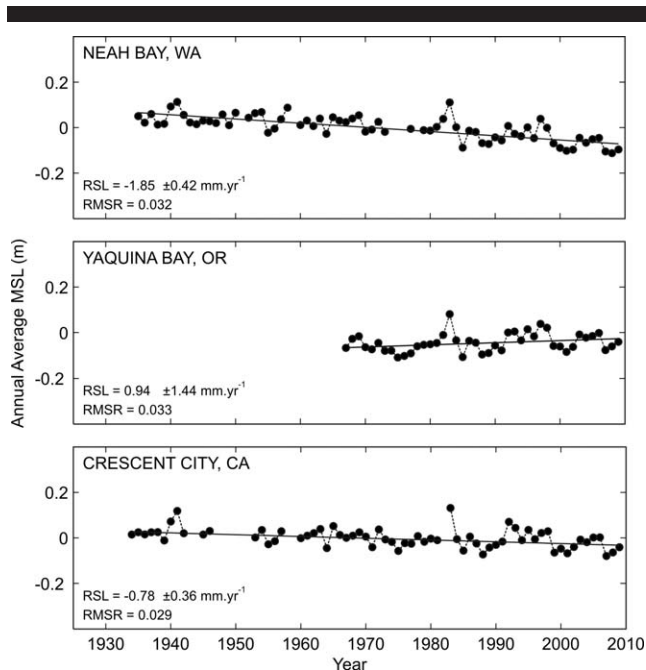


Figure 6. Decadal trends based on the annual average RSLs for the Neah Bay, Yaquina Bay, and Crescent City tide-gauge records, illustrating the alongcoast differences in the trends due to the tectonic effects on land-elevation changes.

which are 0.94 and 1.05 mm/y, respectively. It is evident, however, that the scatter in the data makes these rates uncertain, as is confirmed by the failure of the t-test of their significance, indicating that both are indistinguishable from zero. However, as shown in the following section, analyses limited to the summer reduce the scatter sufficiently so that statistically significant trends are obtained, supporting the basic results found here that increasing RSLs are occurring at those two sites.

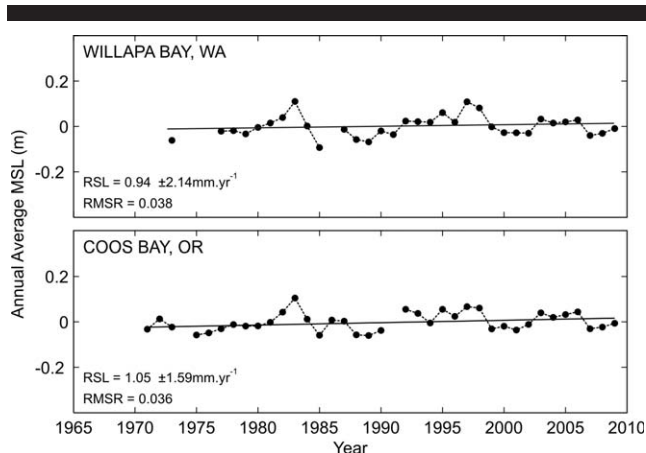


Figure 7. Decadal trends in annual average RSLs for the shorter PNW tide-gauge records from Willapa Bay and Coos Bay.

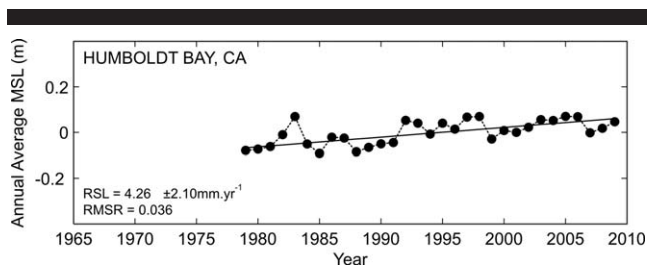


Figure 8. Decadal trends in annual averages for the Humboldt Bay tide gauge, documenting the higher rate of rise in RSLs due to its location nearer the subduction zone and proximity to the Mendocino Fracture Zone.

The graph of the annual averages for Humboldt Bay (Figure 8) shows a pronounced trend of increasing RSLs at a rate of 4.26 mm/y, substantially greater than the eustatic sea-level rise, this stretch of the northern California coast being strongly emergent. As seen in Figures 1 and 2, Humboldt Bay is close to the Mendocino Fracture Zone, where it reaches the coast from offshore and becomes the San Andreas Fault Zone. Humboldt Bay is also significantly closer to the offshore subduction zone than are the other tide-gauge sites. With that proximity, it is expected that when the plates are locked, as they presently are, the deformation of the seaward edge of the continent would result in its down-warping, causing subsidence at this tide-gauge site (shown by local GPS measurements). The release of the strain during a subduction earthquake would result in its immediate uplift. These tectonic controls on the Humboldt Bay tide-gauge site are opposite to the responses at the other PNW tide-gauge sites, accounting for its unusually high rate of increase in the RSL.

It is evident in Figures 6 through 8 that the patterns of scatter in the annual average RSLs above and below the regression lines are closely similar for all coastal gauges. As discussed earlier, this scatter of the data and its alongcoast consistency are due almost entirely to the El Niño–La Niña range of climate events, with El Niños producing the peaks that represent extremes in the annual mean sea levels; most prominent are the peaks in elevated sea levels during the strong 1982–83 and 1997–98 major El Niños. In the longer tide-gauge records analyzed in Figure 6, specifically those from Neah Bay and Crescent City, a cycle is evident in the numbers and levels of the peaks attributed to El Niños. This cycle is the PDO, with shifts between warm and cold phases dominated, respectively, by El Niños and La Niñas. Most evident is the change from cold to warm periods in the mid-1970s, with the strong El Niños having occurred during the recent decades. There is an absence of pronounced peaks during the previous 30- to 40-year cold phase and therefore less scatter in the data to which the regressions have been fitted. This shift in climate in the mid-1970s is also evident in the Yaquina Bay record (Figure 6), but it is seen in Figure 7 that the data from the Willapa Bay and Coos Bay gauges were derived entirely during the warm phase that had strong El Niños such that the scatter dominates the entire lengths of their records, making it difficult to derive statistically meaningful trends for the RSLs.

These assessments of the relative degrees of data scatter based on visual inspections of the graphs are supported by the

statistical analyses included in Table 3. The values for the RMSR, which directly assesses the degrees of data scatter, range from about 0.03 to 0.04 m. The longer tide-gauge records from Neah Bay and Crescent City have values of approximately 0.03 m, whereas the shorter records range more widely in RMSR values but tend to be closer to 0.04 m, reflecting their greater degrees of average scatter. This difference can be attributed mainly to the longer records extending back into the cold phase of the PDO when there was less scatter, whereas the shorter post-1970 records have been significantly affected by the strong 1982–83 and 1997–98 El Niños. This difference can also be seen in the values of the CIs, although the CIs depend directly on the record lengths even after they were corrected for serial correlations. As seen in Table 3, the CI values for Neah Bay and Crescent City are on the order of  $\pm 0.4$  mm/y, whereas those for the short records range roughly from  $\pm 1$  to  $\pm 3$  mm/y, depending largely on their respective lengths, with the shortest record from Port Orford having the largest CI value and thus the greatest uncertainty.

### SUMMER AND WINTER TRENDS, VARIATIONS, AND CLIMATE CONTROLS

While the analyses in the previous section of the trends of annually averaged sea levels based on the long tide-gauge records provided satisfactory assessments of the directions and rates of change in RSLs, the scatter for the shorter tide-gauge records yielded higher uncertainties. It was also evident that the data scatter mostly can be attributed to occurrences of strong El Niños that significantly elevated water levels during the winter, occurrences that are important in our hazard assessments. As was illustrated in Figure 5 for the Seattle tide gauge, separate analyses of the winter and summer records yield results from the winter that provide a better documentation of the extreme water levels during El Niños, whereas the results from the summer minimize the variations caused by both El Niños and storm surges. This section shows that these summer records for the eight coastal gauges, in all but one case, yield improved assessments of the decadal trends in RSLs compared with the results based on annual averages.

The analysis results for three coastal tide-gauge sites, Neah Bay, Yaquina Bay, and Humboldt Bay, are presented in Figure 9, providing examples to illustrate the results from this methodology. Their analyses also represent the range of tectonic effects on the directions and magnitudes in the trends of changing RSLs, discussed in the preceding section based on analyses of the annual averages. It is immediately evident in Figure 9 that this methodology has had its intended effect, documenting the magnitudes of the elevated water levels during El Niño winters while smoothing the summer records to yield improved assessments of the multidecadal trends.

Considering first the summer records, recall that their evaluations included averages of three consecutive months when the water levels are lowest in their seasonal cycle. It is evident from these examples that the scatter remaining in the summer records is fairly uniform over the years at any one site, as well as in comparisons among gauges. Few of the remaining peaks correspond to occurrences of major El Niños, so the cause of the remaining variability is uncertain but likely is the result

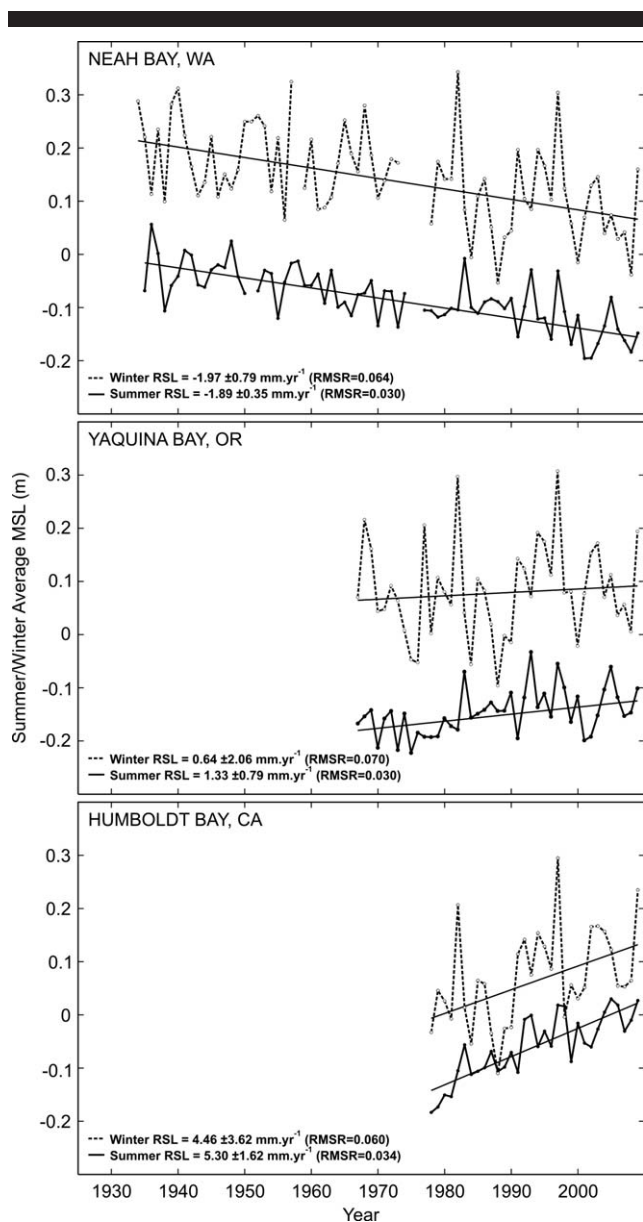


Figure 9. Trends and variations in the winter (dashed lines) versus summer (solid lines) RSLs for the Neah Bay, Yaquina Bay, and Humboldt Bay tide-gauge records.

of year-to-year variations in upwelling and water temperatures. Comparisons in Table 3 between the summer regression statistics and the annual averages presented in the previous section demonstrate that improved trends have been derived by separately analyzing the measured tides during the summer. Again, the simplest assessment of the data scatter is the RMSR, which for the Neah Bay records are respectively 0.032 m and 0.030 m for the analyses of the annual and summer averages (there being only a marginal improvement in this 75-year record by having used the summer data). There has also been a corresponding narrowing of the CI values for the Neah Bay summer record, from  $\pm 0.42$  to  $\pm 0.35$  mm/y. The one

exception to improved results derived by analyzing the summer tides is the record from Crescent City, where the RMSR is somewhat less for the analysis based on the annual averages (0.029 *vs.* 0.039 m), with the CI value similarly narrowed (Table 3); it is uncertain why Crescent City is the one exception.

The distinctions between the analyses of the summer and those of the annual averages are greater for the short tide-gauge records, with analyses based on the summer in all cases yielding improved trends. Most important, for a number of gauges the rates of sea-level change based on the regression slopes differ from those derived from the annual averages, and the CI uncertainties are narrowed for the summer trends (Table 3). These differences are seen, for example, in the statistics for the Yaquina Bay analyses, their trends corrected for the site's instability and subsidence. The 0.94-mm/y rate of increase based on the annual averages increases to 1.33 mm/y when analyzed using the summer data, while the CI narrows from  $\pm 1.44$  to  $\pm 0.79$  mm/y. Later we show that this 1.33-mm/y rate derived from the summer averages closely agrees with the benchmark and GPS surveys of the land-elevation changes. Similar results are obtained for the still shorter records from Willapa Bay, Coos Bay, and Port Orford (Table 3). Although their trends based on the annual averages were all rejected by the t-test as not being statistically different from zero, in the analyses here based on the summer measurements the results for Willapa Bay and Coos Bay are now statistically acceptable, but the 32-year record for Port Orford is still too short to provide confident results. The analysis of the tide-gauge record for Humboldt Bay (Figure 9, bottom) has also been improved using the summer data, with its trend of increasing RSLs rising to 5.30 mm/y and its CI narrowing.

It is clear from these comparisons that in all but one case (Crescent City) the analyses based on the summer records provide improved assessments of the multidecadal trends of changing RSLs. Most important are the results for the short tide-gauge records, with the analyses of the summer months providing significant improvement over the alternative analysis methodologies, including those based on annual averages. In view of these comparisons, the assessments of the trends of changing RSLs derived from the analyses of the summer tide-gauge records are concluded to be the best values for undertaking our assessments of the PNW erosion and flooding hazards.

Our original objective in separately analyzing the summer and winter records was to emphasize the year-to-year variations during the winter to better document the extreme water levels achieved during strong El Niños, and it is evident in Figure 9 that this has been accomplished. Although the statistics for the winter trends were included in Table 3 to provide a complete documentation of our results, they are neither meaningful nor of interest in view of our current focus on the cause of the variations. As already noted in the analyses of the annual average RSLs, there is a close correspondence among the patterns of the scatter found in several tide gauges along the PNW coast, with the most pronounced peaks occurring during the strong El Niños in 1982–83 and 1997–98. This was noted in our earlier study (Allan and Komar, 2006), where we correlated the levels of those peaks above the

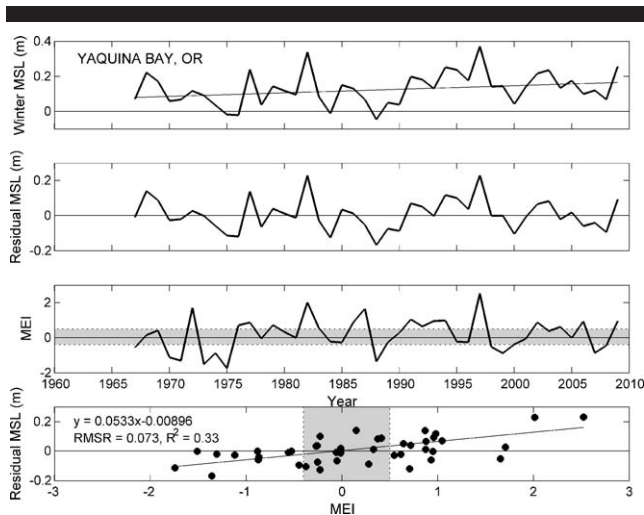


Figure 10. Detrended residual winter water levels for the Yaquina Bay tide-gauge record and their correlation with the MEI.

regression lines (their residuals) with the MEI, demonstrating that the stronger the El Niño, the greater the elevation in the annual average water levels, whereas a La Niña tends to depress the water level. The objective here is to improve that analysis by deriving a correlation between the MEI and the monthly mean water levels during the winter, the season when those levels are highest and most important in contributing to coastal erosion and flooding.

The close correspondence among the winter records from the series of tide gauges is again evident in Figure 9, more so than had been seen in the graphs based on the annual averages. The near congruence for the winter averages in all PNW records is remarkable, demonstrating the high degree of uniform response of the winter-average sea levels to occurrences and ranges in magnitudes of the El Niño–La Niña climate cycles.

The procedure used in our earlier study (Allan and Komar, 2006) to correlate the detrended sea levels with the MEI has been repeated for the winter sea-level records. This procedure is illustrated in Figure 10 for the Yaquina Bay tide gauge. Included is a graph of the MEI values that provide a robust measure of the varying climate from La Niñas to El Niños (Wolter and Timlin, 1993); La Niñas correspond to  $MEI < -0.4$ , El Niños to  $MEI > 0.5$ , with “normal” conditions between (having used an average MEI value that represents the summer and fall conditions, June to November, that precede the winter season when water levels associated with El Niños are elevated). The correspondence between the variations in the measured average winter water levels and the MEI is evident in the upper three panels of Figure 10, while the fourth panel provides a direct correlation between the MEI and the detrended residual water levels for the winter months. The increase in the residuals with the increasing MEI documents that the highest elevated water levels occurred during the strongest El Niños, whereas La Niñas tended to depress the water levels, presumably due to the development of colder, dense water along the coast.

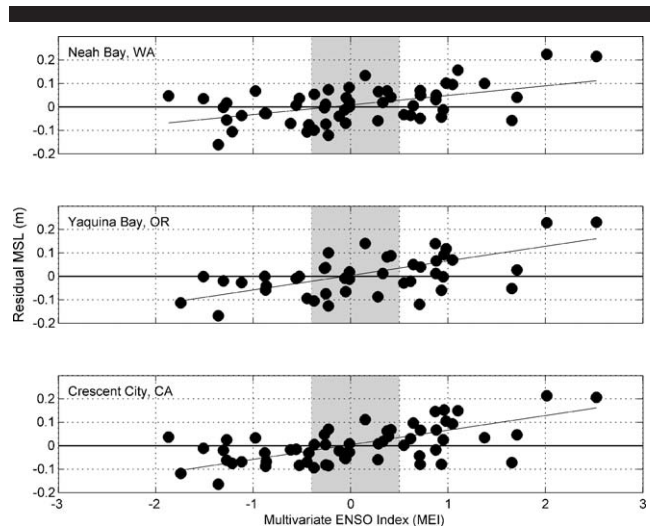


Figure 11. Residual mean winter water levels at Neah Bay, Yaquina Bay, and Crescent City, demonstrating the uniform response along the length of the PNW coast to the range of MEI from La Niñas to strong El Niños.

Similar results were found in analyses of the other PNW tide-gauge records as is apparent in Figure 11, which includes the analyses for Neah Bay and Crescent City, as well as Yaquina Bay. The full range of changes in winter water levels is on the order of 0.4 m, with the strongest El Niños raising the mean water levels by about 0.2 to 0.3 m. This is greater than the total rise in the global mean sea level during the 20th century, demonstrating the significance of El Niños in episodes of PNW coastal property erosion and flooding. The close correspondence of these correlations with MEI for the PNW tide-gauge data analyzed in this study confirms the alongcoast uniformity in the responses of the winter water levels to the ENSO range of climate events.

In our previous study based on the annual average residual water levels, we included tide-gauge records from San Francisco and Los Angeles. We found that similar correlations exist between the water-level residuals and the MEI southward along the California coast (Allan and Komar, 2006). However, in the Los Angeles tide-gauge record, the maximum water levels in the average monthly seasonal cycle occur from August to September, corresponding to the more typical cycle caused by solar warming rather than by coastal upwelling, as occurs in the PNW and along the coast of northern California. Furthermore, the effects of the enhanced water levels during the 1982–83 and 1997–98 major El Niños progressed from south to north, reaching their maxima in Los Angeles in about October, whereas the maxima in the PNW occurred during the following January to February. This earlier occurrence of the El Niño–elevated water levels on the coast of southern California moderates their effects on the resulting erosion, in contrast to the correspondence of the erosion processes in the PNW, where the maximum water levels occur with the major storms and highest waves of winter and when the beaches have been cut back in their seasonal cycles, leaving the shorefront properties more susceptible to erosion impacts (Allan and Komar, 2006).

## ALONGCOAST VARIATIONS IN SEA LEVELS AND LAND ELEVATIONS

In this section, the results from our analyses of the trends of changing RSLs measured by PNW tide gauges are compared with the analyses by Burgette, Weldon, and Schmidt (2009) of land-elevation changes derived from benchmark surveys, undertaken in connection with their investigation of PNW regional tectonics. Comparisons are also made with real-time GPS measurements derived from the Pacific Northwest Geodetic Array (PANGA, 2010), even though those records are relatively short, at maximum 15 years. There are two goals in these comparisons. The first is to establish that these independent data sets are in basic agreement as to their magnitudes and alongcoast patterns of variations, accounting for both submergent and emergent stretches of shore. The second goal is to fill the gaps between our determinations of the RSL trends limited to the tide-gauge sites, providing the RSL values along the entire coast required in our assessments of the erosion and flooding hazards.

Our evaluated summer trends in RSLs for the PNW coastal tide gauges are graphed in Figure 12. The values are listed in Table 3, where their uncertainty bars are the 95% CIs after correcting for serial data correlations. Only the central stretch of the PNW study area is included in this comparison, mainly the coast of Oregon where Burgette, Weldon, and Schmidt (2009) analyzed the land-elevation changes determined from benchmark surveys undertaken during the 1930s and 1980s. To compare the tide-gauge RSL values with the rates of change in land elevations derived from the benchmark surveys, it was necessary to add the regional (eustatic) rate of sea-level rise to the benchmark rates. As demonstrated by the geophysical analyses of Clark, Farrell, and Peltier (1978), the rates of sea-level rise at specific coastal sites can differ significantly from a globally averaged rate, such as the 1.74-mm/y value found by Holgate (2007). The extent of this regional variation in the trends of changing sea levels was shown in the recent review by Cazenave and Llovel (2010), illustrated with satellite data that is now able to document the eustatic water-level changes throughout the world's oceans, although still representing only a short period. Their review also suggested that the nonuniform distribution of the water's temperature increase and thermal expansion is primarily responsible for the spatial patterns of changing sea levels.

Burgette, Weldon, and Schmidt (2009) derived an average rate of  $2.28 \pm 0.20$  mm/y for the PNW regional eustatic component of the sea-level rise, representing the latter half of the 20th century. Their procedure involved several steps based on the Seattle tide-gauge record, with the assumption that it is stable, followed by refined estimates based on the sea-level changes measured by the series of PNW coastal tide gauges; further confirmation came from a comparison with the analyses by Church and White (2006). As graphed in Figure 12, the rates of change in land elevations determined by Burgette, Weldon, and Schmidt (2009) from the benchmarks have been combined with this 2.28 mm/y value for the PNW regional rise in sea level, yielding values for the RSLs that can be compared with our direct assessments derived from the tide-gauge records.

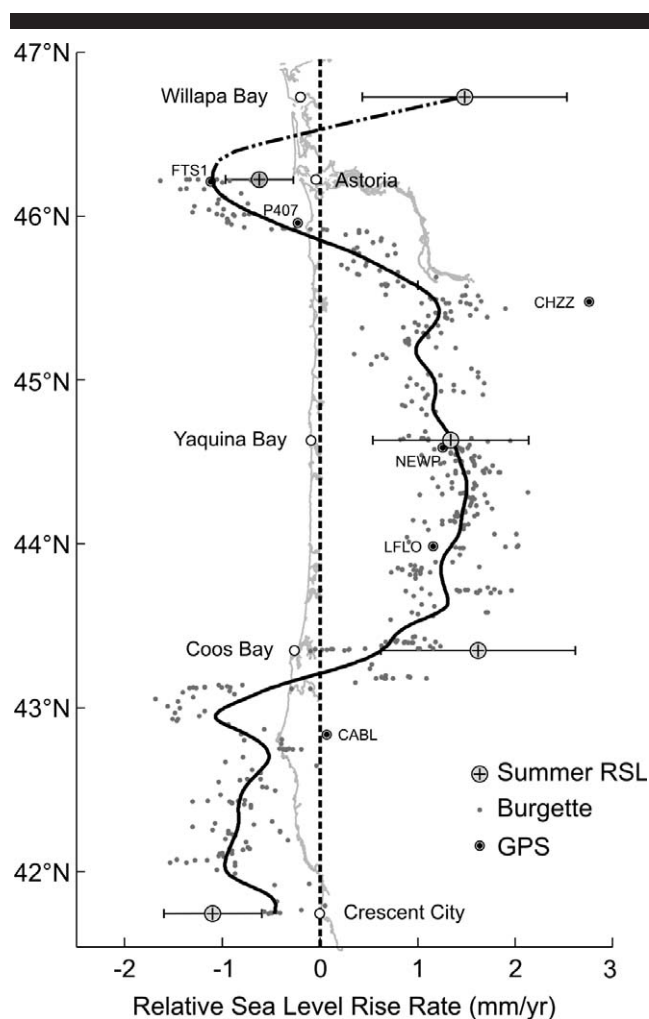


Figure 12. Assessments of changes in RSLs based on tide-gauge records compared with benchmark and GPS measurements of land-elevation changes, with their corresponding RSL rates obtained by adding the 2.28 mm/y PNW eustatic rise in sea level.

The only previous investigation that included the PNW GPS data in comparisons with tide-gauge measurements of RSLs was that by Mazzotti, Jones, and Thomson (2008), which covered the region from Sitka, Alaska, southward along the Canadian west coast and included the PNW south to Crescent City, California. The objective was to account for the land-elevation changes in deriving an assessment for the rise in sea level. Our analysis is the reverse, with the inclusion in Figure 12 of the PANGA real-time GPS measurements of changing land elevations again based on the addition of the 2.28 mm/y eustatic rate for the PNW rise in sea level. There are numerous GPS survey sites throughout the PNW, but most have records spanning only a few years. Our comparisons mostly included GPS sites that are close to the coast and have record lengths of 10 years or greater; however, we did include two 5-year records to better define the pattern of latitude variations graphed in Figure 12. These restrictions yielded seven GPS sites along the coast for our PNW study, with the

northernmost site at Neah Bay, Washington, and the southernmost at Cape Mendocino, California, just south of the Humboldt Bay tide gauge; a 15-year GPS record is also available for Seattle. Six sites along the coast are included in Figure 12 (Fort Stevens, FTS1; Seaside, P407; Cape Mears, CHZZ; Newport, NEWP; Florence, LFLO; and Cape Blanco, CABL). While some of these sites are reasonably close to the tide gauges analyzed in our study, others are located on headlands.

There are uncertainties in the rates of land-elevation changes derived from both benchmarks and GPS records. Figure 12 shows a significant degree of scatter in the benchmark data, amounting to a total spread on the order of 1 mm/y at most latitudes. This scatter is attributed by Burgette, Weldon, and Schmidt (2009) to having largely been caused by the variable distances of the benchmarks from the western edge of the subduction zone. They found in analyses of E–W lines of benchmarks that the magnitude of the land-elevation change is greatest to the W, close to the subduction zone, and progressively decreases inland. The scatter is therefore partly a reflection of the variations in benchmark sites, with their cross-coast (longitude) positions also expected to affect the comparisons with the tide-gauge analyses, depending on their respective locations.

The rates of land-elevation changes derived from the GPS measurements are those provided by the PANGA (2010) linear regressions for each site. However, the overall trends are uncertain, partly because of the shortness of the GPS records and the nonlinearity of their trends that appear to be associated with occurrences of slow-slip (episodic tremor and slip) earthquakes that have been documented in the PNW (*e.g.*, Brudzinski and Allen, 2007; Szeliga *et al.*, 2008). These events are short lived (spanning some 10–20 months) and result in periodic changes to the regional tectonics that produce increased lateral motion, reversals in the predominant direction vectors, and small deformations in the landscape. Thus the combination of short records and nonlinear trends complicates the assessments of the net land-elevation changes derived from the GPS measurements.

The alongcoast patterns in RSLs based on these three independent data sets agree reasonably well, as shown in Figure 12, in view of their scatter and the diverse approaches directed toward evaluating the RSLs. The curve included in the diagram was fitted only to the benchmark data, with smoothing through spatial scales less than approximately 25 km. The benchmarks and GPS data mostly show good agreement, indicating that in general they are obtaining reasonably similar values for the rates of land-elevation changes. Their agreement, in turn, with the tide-gauge assessments of the trends in RSLs implies that the 2.28-mm/y value for the PNW regional eustatic rate of sea-level rise derived by Burgette, Weldon, and Schmidt (2009) is reasonable.

The greatest divergence of the GPS data from the benchmark surveys is found for the Cape Meares (GHZZ) station; the Cape Blanco (CABL) GPS result is marginally different from the benchmark data. Although both sites are characterized by relatively long records (9 and 13 years, respectively), they exhibit nonlinear trends, with steplike increases in GPS elevations that occurred in 2002 and most recently in early

2010. Despite experiencing a recent episode of uplift, the PANGA linear regression of the Cape Meares record yields a net rate of subsidence on the order of  $-0.5$  mm/y, producing the divergent RSL rate of approximately 2.8 mm/y graphed in Figure 12. This apparent occurrence of subsidence at Cape Meares is anomalous for this region that is strongly affected by plate subduction, causing its tectonic uplift that is consistently found in the records from both benchmarks and other GPS sites (NEWP and LFLO) along this stretch of coast. The Cape Meares GPS site is located at the lighthouse on the western edge of the basalt headland, but this headland is bounded by faults. There is also geologic evidence suggesting that the GPS site may be on a translational landslide that is slowly moving seaward and presumably downward. Whatever the cause, it is likely that the Cape Meares GPS site is unstable, accounting for its anomalous record and the deviant value of RSL graphed in Figure 12.

South of Coos Bay along the southern Oregon coast, the benchmark data show a significant degree of scatter (Figure 12). However, their measured rates of uplift are on the order of 3 mm/y, greater than the 2.28-mm/y regional eustatic rate, so this stretch of coast is emergent. The Cape Blanco (CABL) GPS site yields a lower rate of uplift, 2.2 mm/y, which is essentially the same as the regional eustatic rate of rising sea level such that the evaluated net RSL change is effectively zero. The closest tide gauge is located in Port Orford (Figure 2), with a measured RSL change of 1.47 mm/y for the summer record. This clearly contradicts the benchmark data for this portion of the southern Oregon coast. However, as indicated in Table 3, the trends for the Port Orford tide gauge are not statistically significant; the CI estimates exceed the actual trend, likely due to the large number of missing data points. For these reasons, its trend has been omitted from Figure 12. Farther south, at the latitude of Crescent City, the assessment of the RSL trend based on the tide-gauge record agrees with the benchmark data, indicating that this is an emergent stretch of shore due to the high rate of tectonic uplift. However, the tide-gauge record implies a higher rate of increasing land elevations than recorded by the benchmarks at that latitude. This difference is likely a result of the E–W variations in the tectonic uplift analyzed by Burgette, Weldon, and Schmidt (2009), with the tide gauge located on the open coast within the harbor's breakwater, whereas the benchmarks are farther inland.

On the central Oregon coast, the 1.33-mm/y rate of rise in the RSL based on the Yaquina Bay summer tide-gauge record agrees closely with both benchmark and GPS (NEWP and LFLO) data (Figure 12). This portion of the coast is submergent, even though it is tectonically rising. This 1.33-mm/y rate for the Yaquina Bay tide gauge is the value corrected for the subsidence of that gauge's primary benchmark, as reported by Burgette, Weldon, and Schmidt (2009); without that correction, the evaluated rate would have been 2.78 mm/y, in marked disagreement with the benchmark and GPS data.

The clearest example of the significance of the inland decrease in the rates of tectonic uplift is found along the Columbia River, where the tide gauge is inland at Astoria but the benchmarks and GPS station are closer to the coast. As seen in Figure 12, the result is that the change in RSL measured by the tide gauge is on the order of  $-0.5$  mm/y, whereas those

derived from the benchmarks and GPS station are approximately  $-1$  mm/y due to their higher rates of tectonic uplift. Burgette, Weldon, and Schmidt (2009) confirmed this response through an analysis of an E–W line of benchmarks directed upriver, which demonstrated that the magnitude of land-elevation change is greatest to the W, on the coast, and progressively decreases inland.

In this example with the Astoria tide-gauge analysis having yielded a different assessment of the change in RSL than the benchmarks and GPS station, in the application to our coastal hazard assessments the  $-1.0$  to  $-1.2$  mm/y rates of decreasing RSL based on the benchmark resurveys would be more relevant than the result from the Astoria tide gauge located inland. However, for other sites the tide-gauge results would be expected to correspond more closely to the RSL trend experienced along the ocean shore, Crescent City being an example in which the benchmark data represent inland positions.

The combined results in Figure 12, derived from our tide-gauge analyses and from the benchmark and GPS land-elevation measurements, document the alongcoast variations in directions and magnitudes in RSLs, with stretches of both submergent and emergent shores. There is a marked transition near the latitude of Coos Bay, with an emergent shore to its south where the rate of lowering RSL is on the order of  $-1$  mm/y. In contrast, there is a stretch of submergent shore along the length of the central Oregon coast, represented by an RSL rise of about  $1.25$  mm/y. Farther north, the transition from submergent to emergent shores occurs approximately at Tillamook Head, immediately north of the community of Cannon Beach ( $45^{\circ}53'$ ). Here, the presence of heavy vegetation on the sea cliff and the absence of a history of erosion support the conclusion that this shore is reasonably stable (Komar and Shih, 1993), as indicated by the benchmark data and the GPS site (P407) nearby at Seaside.

Although not included in Figure 12, comparisons along the Washington coast between our assessments of RSLs from the tide-gauge records and nearby GPS sites show good agreement. They document the high rates of tectonic uplift along the northern Washington coast to Neah Bay, resulting in downward trends of changing RSLs, that shore being strongly emergent. Reasonable agreement is also found along the coast of northern California, specifically between the tide-gauge result from Humboldt Bay and the Cape Mendocino GPS site, confirming the tectonic-induced subsidence of that shore and its resulting high rate of increasing RSL. These alongcoast variations in land-elevation changes and trends in RSLs derived from the tide gauges have been interpreted by Burgette, Weldon, and Schmidt (2009) to be a result of segmented plate subduction, the variations in the slopes and depths of the descending ocean plates within the subduction zone.

## SUMMARY AND DISCUSSION

The objective of this study was to analyze the progressive multidecadal trends and monthly to annual variations in mean sea levels along the coast of the U.S. PNW, the ocean shores of Washington, Oregon, and northern California. These assessments are a fundamental component in our development of

coastal erosion and flooding hazard zones, both to represent the present-day environmental conditions and to project those hazards into the future. The sea-level analyses were based on eight tide gauges covering the length of this coast, as well as the long-term Seattle gauge within Puget Sound, which was used to develop our analysis methodologies.

The trends in RSLs measured by the gauges are strongly affected by the tectonics of this region, the collision and subduction of the oceanic Juan de Fuca and Gorda plates beneath the continental North American plate. The active tectonics have resulted in significant alongcoast variations in land-elevation changes and trends of RSLs that range from  $-1.89$  mm/y on the emergent shore of Neah Bay on the north coast of Washington, to the submergent shore along the north-central Oregon coast, with an RSL rise of  $1.33$  mm/y determined from the Yaquina Bay tide gauge. Another stretch of emergent coast exists south of Coos Bay to Crescent City, California, where the rate of lowered RSL is  $-1.10$  mm/y. The highest rate of rising RSL occurred at Humboldt Bay in northern California ( $5.30$  mm/y), being the only area along the PNW coast where land elevations are dropping as stress accumulates between the locked tectonic plates. These alongcoast variations in the directions and magnitudes of the RSLs evaluated from the tide-gauge records are in reasonable agreement with the data for land-elevation changes along this coast—the measurements derived from benchmark surveys analyzed by Burgette, Weldon, and Schmidt (2009), and the real-time GPS measurements close to the coast. The combination of these data sets, presented in Figure 12, documents the latitude variations in RSLs that will be used in our assessments of the erosion and flooding hazards along the PNW coast.

Also important to the hazard assessments are the ranges in the monthly and annual variations in mean sea levels, particularly the extreme water levels that occur during strong El Niños, such as those in 1982–83 and 1997–98. During those climate events, the winter monthly mean water levels were some 50 cm higher than during the preceding summer and 20 to 30 cm higher than the winter water elevations during normal (non-El Niño) winters. A new methodology was developed to serve as the basis for assessments of the magnitudes of the El Niño-elevated water levels. This methodology involved separate evaluations for winter and summer—averages of the highest three months of the winter and lowest three months of the summer. The resulting pair of seasonal linear regressions for each tide gauge shows a consistent difference in the mean water levels over the years, being highest during the winters, reflecting the total magnitude in the seasonal cycle of monthly mean water levels. The primary objective of this analysis methodology was to show that the winter records emphasize the extreme water levels during strong El Niños, which permitted the development of a predictive correlation with the MEI that represents the range of climate events from La Niñas to strong El Niños. The results are consistent for all tide gauges along the PNW coast, with the highest water levels occurring during the strongest El Niños, whereas the formation of cold, dense water during a La Niña tends to depress the water levels along this coast.

An important by-product of this methodology to separately analyze the winter and summer sea-level records was that the

scatter in the summer monthly mean levels is smoothed by eliminating essentially all variations from year to year due to the El Niño–La Niña cycles, as well as the effects of storms. This yielded our best assessments of the multidecadal trends in RSLs. With these improved assessments of the progressive trends and extremes in the winter monthly averages caused by El Niños, our analyses documented the primary water level controls that are important in the hazard assessments. Research is under way to investigate the third component, the occurrences and magnitudes of storm surges, including analyses of their potential climate controls.

In parallel with our investigations of the PNW sea levels are analyses of its ocean wave climate, based on NOAA wave-buoy data collected since the mid-1970s. Our earlier investigations discovered that the measured significant wave heights have been progressively increasing due to the occurrence of stronger storms (Allan and Komar, 2000, 2006). Our most recent investigation extended those analyses to document the degree to which the largest measured waves generated by the most severe storms have been increasing at the highest rates, leading to improved assessments of extreme-wave projections needed in the hazard assessments (Ruggiero, Komar, and Allan, 2010). The ultimate goal of this research is to combine these processes, the measured tides and sea levels with the increasing deep-water wave heights and parallel increases in breaking waves and swash run-up elevations on the PNW beaches, to account for the climate controls on these processes and to derive improved assessments of future erosion and flooding hazards, which are projected to significantly increase in future decades.

### ACKNOWLEDGMENTS

This study has been supported by the Sectoral Applications Research Program of the U.S. Department of Commerce (NOAA) under grant NA08OAR4310693. We thank our students, Heather Baron and Erica Harris, for their assistance in aspects of this study of the PNW hazards. Thanks also to the reviewers of this paper for their helpful suggestions.

### LITERATURE CITED

- Allan, J.C. and Komar, P.D., 2000. Are ocean wave heights increasing in the eastern North Pacific? *EOS, Transaction of the American Geophysical Union*, 81(47), 561, 566–567.
- Allan, J.C. and Komar, P.D., 2006. Climate controls on U.S. West Coast erosion. *Journal of Coastal Research*, 22(3), 511–529.
- Atwater, B.F., 1987. Evidence for great Holocene earthquakes along the outer coast of Washington state. *Science*, 236, 942–944.
- Atwater, B.F. and Hemphill-Haley, E., 1997. Recurrence Intervals for Great Earthquakes of the Past 3500 Years at Northeastern Willapa Bay, Washington. U.S. Geological Survey Professional Paper 1576, 108p.
- Bindoff, N.L.; Willebrand, J.; Artale, V.; Cazenave, A.; Gregory, J.; Gulev, S.; Hanawa, K.; Le Quééré, C.; Levitus, S.; Nojiri, Y.; Shum, C.K.; Talley, L.D., and Unnikrishnan, A., 2007. Observations: oceanic climate change and sea level. In: Solomon, S.; Qin, D.; Manning, M.; Chen, Z.; Marquis, M.; Avery, K.B.; Tignor, M., and Miller, H.L. (eds.), *Climate Change 2007: The Physical Science Basis*. Contribution of Working Group I to the Fourth Assessment Report of the Intergovernmental Panel on Climate Change. Cambridge, United Kingdom: Cambridge University Press, pp. 385–432.
- Burdzinski, M. and Allen, R.M., 2007. Segmentation in episodic tremor and slip all along Cascadia. *Geology*, 35(10), 907–910.
- Burgette, R.J.; Weldon, R.J., and Schmidt, D.A., 2009. Interseismic uplift rates for western Oregon and along-strike variation in locking on the Cascadia subduction zone. *Journal of Geophysical Research*, 114, B01408, doi: 10.1029/2008JB005679.
- Cazenave, A. and Llovel, W., 2010. Contemporary sea-level rise. *Annual Review of Marine Science*, 2, 145–173.
- Church, J.A. and White, N.J., 2006. A 20th century acceleration in global sea-level rise. *Geophysical Research Letters*, 33, L01602, doi:10.1029/2005GL024826.
- Clark, J.A.; Farrell, W.E.; and Peltier, W.R., 1978. Global change in post-glacial sea level: a numerical calculation. *Quaternary Research*, 9, 265–287.
- Douglas, B.C., 2001. Sea level change in the era of the recording tide gauge. In: Douglas, B.C.; Kearney, M.S., and Leatherman, S.P. (eds.), *Sea Level Rise, History and Consequences*. International Geophysics Series, Volume 75. New York: Elsevier, pp. 37–64.
- Goldfinger, C.; Nelson, C.H.; Morey, A.; Johnson, J.E.; Gutierrez-Pastor, J.; Ericsson, A.T.; Karabanov, E.; Patton, J.; Gracia, E.; Enkin, R.; Dallimore, A.; Dunhill, G., and Vallier, T., in press. Turbidite Event History: Methods and Implications for Holocene Paleoseismicity of the Cascadia Subduction Zone. U.S. Geological Survey Professional Paper 1661-F, Reston, Virginia.
- Hansen, J.E., 2007. Scientific reticence and sea level rise. *Environmental Research Letters*, 2, 024002, doi:10.1088/1748-9326/2/2/024002.
- Holgate, S., 2007. On the decadal rates of sea level change during the twentieth century. *Geophysical Research Letters*, 34, 1–4.
- Huyer, A., 1977. Seasonal variations in temperature, salinity, and density over the continental shelf off Oregon. *Limnology and Oceanography*, 22, 442–453.
- Huyer, A. and Smith, R.L., 1985. The signature of El Niño off Oregon, 1982–83. *Journal of Geophysical Research*, 90(C4), 7133–7142.
- Inman, D.L. and Nordstrom, C.E., 1971. On the tectonic and morphological classification of coasts. *Journal of Geology*, 79, 1–21.
- Kelsey, H.M.; Nelson, A.R.; Hemphill-Haley, E., and Witter, R.C., 2005. Tsunami history of an Oregon coastal lake reveals a 4600 yr record of great earthquakes on the Cascadia subduction zone. *Geological Society of America Bulletin*, 117(7/8), 1009–1032.
- Komar, P.D., 1997. *The Pacific Northwest Coast*. Durham, North Carolina: Duke University Press.
- Komar, P.D. and Shih, S.M., 1993. Cliff erosion along the Oregon coast: a tectonic–sea level imprint plus local controls by beach processes. *Journal of Coastal Research*, 9, 747–765.
- Leonard, L.J.; Currie, C.A.; Mazzotti, S., and Hyndman, R.D., 2010. Rupture area and displacement of past Cascadia great earthquakes from coastal coseismic subsidence. *Geological Society of America Bulletin*, 122(11/12), 1951–1968.
- Maul, G.A. and Martin, D.M., 1993. Sea level rise at Key West, Florida, 1846–1992: America's longest instrument record? *Geophysical Research Letters*, 20, 1955–1958.
- Mazzotti, S.; Jones, C., and Thomson, R.E., 2008. Relative and absolute sea level rise in western Canada and northwestern United States from a combined tide gauge–GPS analysis. *Journal of Geophysical Research*, 113(CC11019), 19p, doi:10.1029/2008JC004835.
- Miller, L. and Douglas, B.C., 2004. Mass and volume contributions to twentieth-century global sea level rise. *Nature*, 428, 406–409.
- Mitchell, C.E.; Vincent, P.; Weldon, R.J., and Richards, M.A., 1994. Present-day vertical deformation of the Cascadia margin, Pacific Northwest, United States. *Journal of Geophysical Research*, 99(B6), 12257–12277.
- Nelson, A.R.; Kelsey, H.M., and Witter, R.C., 2006. Great earthquakes of variable magnitude at the Cascadia subduction zone. *Quaternary Research*, 65, 354–365.
- NOS (National Ocean Service), 2009. NOAA Tides and Currents: Center for Operational Oceanographic Products and Services. <http://www.co-ops.nos.noaa.gov/> (accessed April 1, 2010).
- PANGA (Pacific Northwest Geodetic Array), 2010. Central Washington University. Real-Time GPS Data Analysis. <http://www.geodesy.cwu.edu/realtime/> (accessed August 1, 2010).

- Pfeffer, W.T.; Harper, J.T., and Neel, S.O., 2008. Kinematic constraints on glacier contributions to 21st century sea-level rise. *Science*, 321, 1340–1343.
- Pugh, D., 2004. *Changing Sea Levels: Effects of Tides, Weather and Climate*. Cambridge, UK: Cambridge University Press, 255p.
- Ruggiero, P., 2008. Impacts of climate change on coastal erosion and flood probability in the US Pacific Northwest. In: *Proceedings of the Solutions to Coastal Disasters Conference* (Oahu, Hawaii), pp. 158–169.
- Ruggiero, P.; Komar, P.D., and Allan, J.C., 2010. Increasing wave heights and extreme-value projections: the wave climate of the U.S. Pacific Northwest. *Coastal Engineering*, 57(5), 539–552, doi:10.1016/j.coastaleng.2009.12.005.
- Satake, K.; Shemazaki, K.; Yoshinobu, T., and Ueda, K., 1996. Time and size of a giant earthquake in Cascadia inferred from Japanese tsunami records of January 1700. *Nature*, 379(6562), 246–249.
- Smith, R.L.; Huyer, A., and Fleischbein, J., 2001. The coastal ocean off Oregon from 1961 to 2000: is there evidence of climate change or only Los Niños? *Progress in Oceanography*, 49, 63–93.
- Szeliga, W.; Melbourne, T.; Santillan, M., and Miller, M., 2008. GPS constraints on 34 slow slip events within the Cascadia subduction zone 1997–2005. *Journal of Geophysical Research*, 113, B04404.
- Witter, R.C.; Kelsey, H.M., and Hemphill-Haley, E., 2003. Great Cascadia earthquakes and tsunamis of the past 6700 years, Coquille River estuary, southern coastal Oregon. *Geological Society of America Bulletin*, 115, 1289–1306.
- Wolter, K. and Timlin, M.S., 1993. Monitoring ENSO in COADS with a seasonally adjusted principal component index. In: *17th Climate Diagnostic Workshop* (Climatology Survey, CIMMS and the School of Meteorology, University of Oklahoma), pp. 52–57.
- World Meteorological Organization, 1966. Climate Change: Report of a Working Group on the Commission for Climatology. Technical Note 79, 79p.
- Zervas, C., 2001. Sea Level Variations of the United States 1854–1999. National Oceanic and Atmospheric Administration Technical Report NOS CO-OPS 36. Silver Spring, Maryland: NOAA, 80p.
- Zervas, C., 2009. Sea Level Variations of the United States 1854–2006. National Oceanic and Atmospheric Administration, Technical Report NOS CO-OPS 053. Silver Spring, Maryland: NOAA, 78p.